



2nd Canada-US CanSmart Workshop

SMART MATERIALS AND STRUCTURES

10 - 11 October 2002, Montreal, Quebec, Canada.

AN X-RAY DIFFRACTION STUDY OF PMN-PT CERAMICS IN THE REGION OF THE RELAXOR TRANSITION

H.W. King and S.H. Ferguson

University of Victoria, Department of Mechanical Engineering
Victoria, BC

D.F. Waechter and S.E. Prasad

Sensor Technology Ltd.
Collingwood, ON

ABSTRACT

Electrostrictive ceramics in the solid solution $(1-x)\text{PMN}-x\text{PT}$ can be used to fabricate high strain actuators for smart structure applications. For example, multi-layer actuators fabricated from 0.9PMN-0.1PT have exhibited over twice the displacement capability of similar actuators made from a soft PZT having $d_{33}=580$ pC/N (Waechter et al., 2000). To assist in the development of other compositions, the relaxor region of the phase diagram of the PMN-PT system has been investigated by high temperature X-ray diffraction using ceramics with compositions $x = 0.00, 0.08$ and 0.20 .

Lattice parameter measurements show that the thermal expansion coefficients of the samples increase by an order of magnitude at a well defined temperature T_{α} . Diffraction profile studies show that T_{α} can be correlated with the onset of the cubic-pseudocubic transformation, with its associated microregions of polarization. The profile studies also indicate that the onset of the low temperature stable rhombohedral phase can be correlated with the temperature at which remanent polarization ceases to exist. A tentative phase diagram for the relaxor region of the PMN-PT ceramic system is developed on the basis of these findings.

INTRODUCTION

Electrostrictive ceramics in the perovskite solid solution system PMN-PT, where PMN refers to $\text{Pb}(\text{Mg}_{1/3}\text{Nb}_{2/3})\text{O}_3$ and PT to PbTiO_3 , are relaxor perovskites that exhibit

a diffuse paraelectric to ferroelectric transition which enables high voltage-induced strains to be achieved with little or no hysteresis. These materials fill a much needed gap in the electromechanical properties of $\text{PbZrO}_3\text{-PbTiO}_3$ (PZT) piezoelectrics, since hard PZTs exhibit low hysteresis, but have small values of d_{33} , while the softer PZTs have higher values of d_{33} , but exhibit larger hysteresis. Ceramic elements fabricated from 0.9PMN-0.1PT have exhibited a strain of over 0.12% at a field of 3.5 MV/m (Waechter et al., 2000). The PMN-PT ceramics are thus well suited for use as actuators in smart structure systems that require precise and highly reproducible displacements.

In contrast to piezoelectric ceramics, the dielectric constant of relaxors does not exhibit a sharp peak at a well defined temperature T_c , but passes through a shallow maximum at a temperature T_m . The temperature of this dielectric peak is sensitive to both the composition of the sample and the frequency of the applied field. Choi et al. (1989) and Feigelson (2002) have published dielectric property diagrams for the PMN-PT ceramic system using dielectric property data. Although these diagrams are not based on crystallographic investigations, the regions between the property-temperature plots are labeled in terms of crystal structures, so the plots are commonly referred to as "phase diagrams" (see, for example, Zhang et al. 1996). In the relaxor region of the PMN-PT system, which occurs below about 30 mol.% PT, the boundary between the cubic and rhombohedral perovskite phases is based on the compositional dependence of T_m , determined at a standard frequency of 1 kHz. It is known, however, that the saturation polarization in relaxors does not go to zero until a temperature greater than T_m (see, for example, Cross, 1994). The use of T_m as a parameter to define the temperature of the ferroelectric transition has been questioned by Burns and Dacol (1983), who have inferred the presence of randomly oriented regions of polarization in PMN at temperatures as high as 344 °C, based on observations of deviations from the linear temperature dependence of the optical refractive index. On the other hand, Viehland et al. (1990, 1991), have suggested the use of a lower temperature parameter T_f , below which relaxors display a remanent polarization. In this context, many authors have also commented on the absence of a reduction in macrosymmetry on cooling relaxors through T_m (Guisheng et al., 2000, Ye et al. 1993, Westphal et al. 1992, de Mathan et al., 1991 and Schmidt, 1990) and the retention of pseudocubic symmetry and optical isotropy at temperatures down to 4 K (Schmidt, 1992).

Ho et al. (1993) investigated the structural phases in PMN-PT system using high temperature X-ray diffraction, but focused their attention on higher compositions in the region of the morphotropic phase transformation. They examined only one sample in the relaxor region, containing 29 mol.% PT, and reported no changes in the pseudocubic diffraction pattern on heating through T_m . In a low temperature examination of the structure of PMN by X-ray and neutron scattering, de Mathan et al., (1991) found broadened peaks of the pseudocubic structure at temperatures down to 5 K. Guisheng et al. (2000) found that a composition of 0.76PMN-0.24PT displayed more normal ferroelectric characteristics, compared to the relaxor properties of PMN. They also

reported peak splitting in the room temperature diffraction pattern of this sample, which they attributed to the cubic to rhombohedral transformation, but did not identify a temperature for the phase transformation by X-ray diffraction. In a preliminary high temperature X-ray diffraction study of PMN-PT ceramics, the present authors (King et al., 2002) found no change in the pseudocubic diffraction pattern when a powder sample of 0.9PMN-0.1PT was slowly heated, or cooled, through its T_m temperature of 38 °C. However, high temperature lattice parameter measurements on the same sample showed that an order of magnitude increase in thermal expansion coefficient occurs at a temperature about 80-100 °C above T_m . In early studies, Smolenski and coworkers (1961A,B) frequently measured the temperature dependence of the thermal expansion coefficient (α), which was regarded as a prime indicator of the ferroelectric transition, but in PMN they found only a shallow minimum in α in the region of its T_m of -18 °C (1961C). However, a marked increase in α was observed (but not commented upon) at higher temperatures in the region of room temperature. Significant lattice softening has also been reported in PMN by Cross (1987), who attributed it to the persistence of micropolar regions at temperatures above T_m . In view of these confusing interpretations and practices with respect to the PMN-PT phase diagram, a range of compositions across the system is being investigated by high temperature X-ray diffraction. The results obtained for ceramics with compositions in the relaxor region are presented at this workshop.

EXPERIMENTAL METHODS

Specimens of (1-x)PMN-xPT, with compositions of $x = 0.00, 0.08$ and 0.20 were fabricated at Sensor Technology Ltd., Collingwood, ON, using a direct synthesis technique. As described previously by Waechter et al.(2000), this single calcination process is considerably less complex and expensive than the commonly used two-step columbite process (Swartz, 1984). Proportionate amounts of the oxides of lead, magnesium and niobium to give the required compositions were ball milled to fine powder and calcined to form the mixed oxide perovskite phase. The homogeneous product was further crushed and milled to fine powder, and then pressed into discs about 25 mm diameter and 1.2 mm thick. After bisquing to remove volatile organic binders and lubricants, the disks were fired to obtain sintered ceramics, which were ground flat and then cut into X-ray specimens 12.5 mm wide x 19 mm long x 1 mm thick.

X-ray diffraction experiments were performed on a Scintag XDS 2000 theta-theta X-ray diffractometer equipped with a high resolution Peltier-cooled drifted Si detector and operated at 44 kV and 40 mA using copper radiation ($\lambda_{CuK\alpha 1} = 1.54060 \text{ \AA}$). A Buehler HDK2.3 high temperature attachment was used for controlling sample temperatures between room temperature and 300°C. The samples were mounted on a specially designed stainless steel sample holder which was rigidly clamped at one end only, to permit free expansion in the plane of the specimen. To eliminate thermal gradients along the length of the specimen, the sample was heated in air using only the

surround heater of the Buehler furnace and its temperature was measured and controlled to ± 1 °C, using a Pt/Pt-13%Rh (type S) thermocouple. Cryogenic temperatures down to -70 °C were obtained with an MMR Technologies cryogenic cold finger, cooled by the Joule-Thompson effect using high pressure nitrogen. As described elsewhere (King et al., 1994). The cold finger was mounted on a flange plate fitted to the Buehler high temperature vacuum chamber. The temperature was measured by a silicon diode sensor embedded in the sample mount and controlled to ± 0.2 °C by offsetting the cryogenic cooling using a Si resistance heater, which was also embedded in the sample mount. Temperatures between room temperature and 100 °C were obtained by using the heater, without introducing the cryogenic cooling gas. A vacuum of at least 10^{-3} Torr was used to provide thermal insulation and also to prevent condensation of water vapour onto the cold sample surface.

For lattice parameter determinations, at least nine relatively intense Bragg peaks of the perovskite structure over the angular range from 60 to 141 °2 θ were step scanned using a receiving slit of 0.3°, a step size of 0.06° with a dwell time of 2.5 seconds. To eliminate angular dependent instrumental and measurement errors, lattice parameters calculated from the Bragg peak positions were plotted against the function $\cos\theta*\cot\theta$ and extrapolated to $\theta = 90^\circ$. An equation for the linear line trend was derived for each of these plots, to obtain a lattice parameter with an estimated accuracy of ± 0.0001 Å (King and Payzant, 2001). For the investigation of crystal structure changes by Bragg peak splitting, a selected diffraction profile was step-scanned with a much longer dwell time of 20 seconds, using the same step size of 0.06°, to reduce the scatter of the results.

RESULTS

Temperature Dependence of Lattice Parameters

The room temperature X-ray diffraction patterns obtained for the three PMN–PT samples are given in Fig. 1. All show Bragg peaks of the pseudocubic structure, which are broadened so that the $K_{\alpha 1}$ and $K_{\alpha 2}$ peaks are not clearly resolved at Bragg angles below 90 °2 θ . The absence of a significant diffraction peak in the region of 29 °2 θ confirmed that the ceramic samples are effectively free of the pyrochlore phase.

The lattice parameters determined at 20 °C intervals over the temperature range from -50 to +300 °C, are plotted against temperature in Fig. 2. None of the plots show any deviation from a strictly linear trend at their respective T_m temperatures of -18, 32 and 93 °C, taken from the diagrams of Choi et al. (1989) and Feigelson (2002). At relatively low temperatures, all of the lattice parameter vs. temperature plots have very shallow slopes, consistent with a thermal expansion coefficient (α) of the order of 10^{-6} mm/mm per °C. The PMN result is consistent with the earlier finding of Smolenski et al. (1961C), who did not detect a significant change in α at the T_m temperature of -18 °C. However, all of the lattice parameter plots in Fig. 2 show a very significant increase in

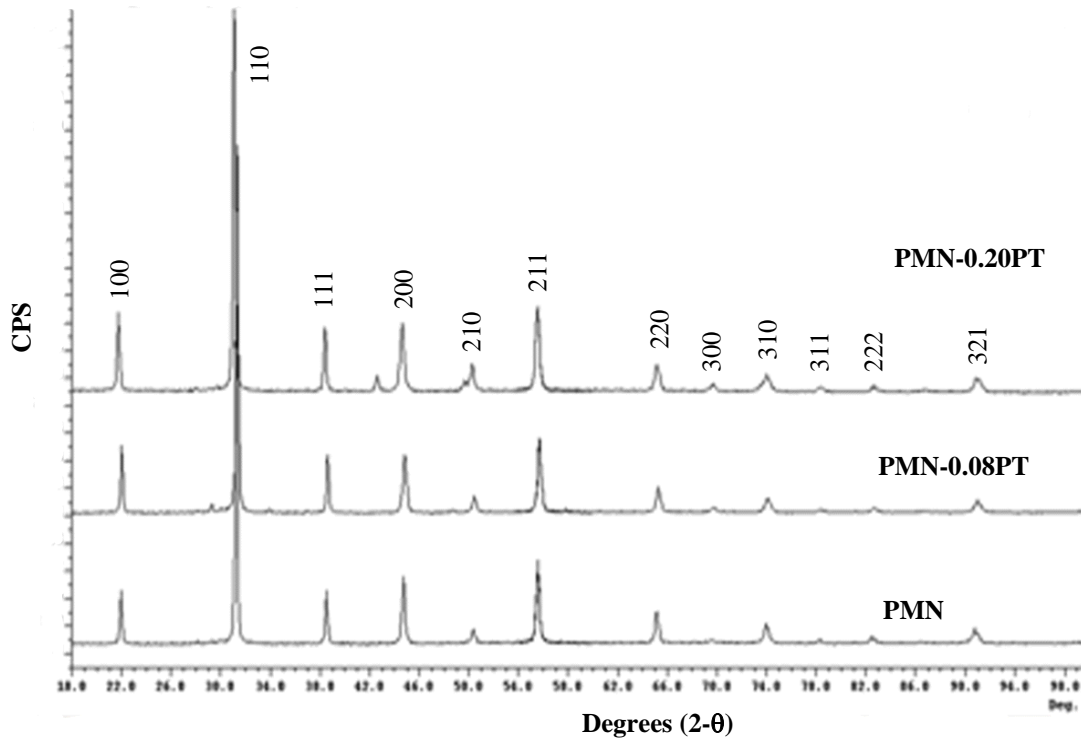


Figure 1. Peaks for (1-x)PMN-xPT where x= 0.00, 0.08 and 0.20

slope on heating above a well defined temperature labeled T_{α} , so that the thermal expansion coefficients are increased by an order of magnitude, to the level of 10^{-5} mm/mm per °C. It is significant to note that the increase in the thermal expansion coefficient of PMN is of the same order as that reported by Cross (1987) for PMN, though the softening temperature of $T_{\alpha} = 103$ °C is not quite as high as the equivalent temperature he obtained by a linear extrapolation. The T_{α} temperatures of 112 and 138 °C obtained for the 0.92PMN-0.08PT and 0.8PMN-0.2PT samples are considerable greater than the respective T_m values of 32 and 93 °C.

Temperature Dependence of Diffraction Profiles

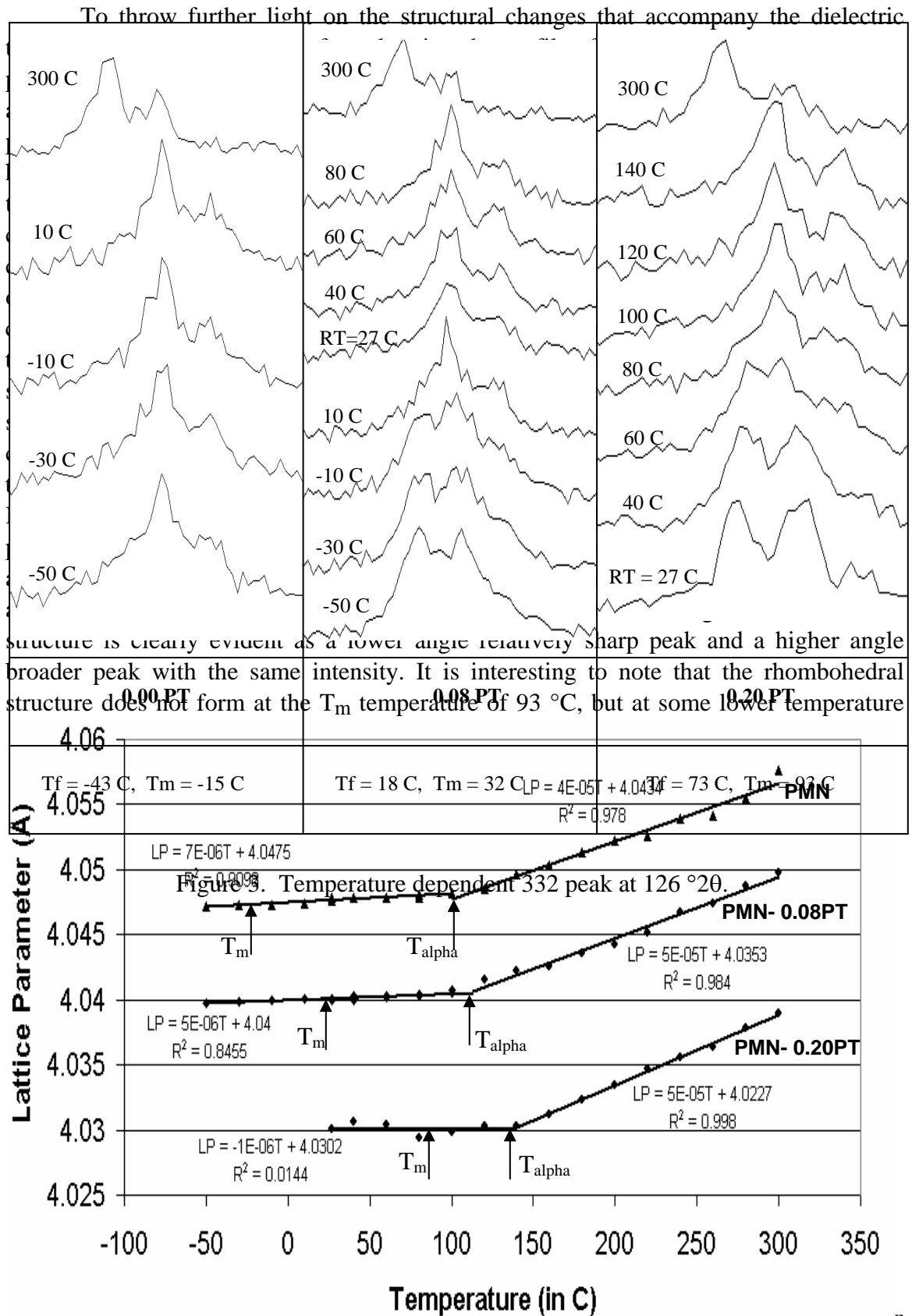


Figure 2. Lattice Parameters vs. Temperature for (1-x)PMN-xPT.

between 80 and 60 °C. A similar structural trend was evident from the diffraction patterns obtained during the cooling of the 0.92PMN-0.08PT sample. The broadened cubic 322 peak is observed at temperatures down to room temperature, while the rhombohedral diffraction pattern appears between +10 and -10 °C. Again, it is significant to note that the onset of the rhombohedral phase does not occur until a temperature below the T_m of 32 °C. In the PMN sample, the broadened pseudocubic peaks are observed on cooling down to -30 °C, but on further cooling to -50 °C the profile shows additional broadening in the $K_{\alpha 2}$ region, indicating that the onset of the rhombohedral phase occurs at a temperature below the T_m of -18 °C. Additional profile broadening in PMN was observed in this angular region by de Mathan et al. (1991) and their data also shows two equal intensity peaks in this region at 5 K.

The temperature of the structural transformation cubic to pseudocubic is more difficult to assess, as the cubic diffraction profiles are strain broadened due to the pressing-sintering treatment used to fabricate the ceramics. Referring again to the 0.8PMN-0.2PT sample, the cubic 332 peak shows additional broadening, particularly in the vicinity of the $K_{\alpha 2}$ peak, on cooling between 140 and 120 °C. Similar broadening in the vicinity of the $K_{\alpha 2}$ peak of the 0.92PMN-0.08PT sample can be observed at 80 °C, but as there are no profile measurements at higher temperatures below 300 °C, the precise temperature of the onset of broadening cannot be determined from the present results. A similar lack of profile data between 10 °C and 300 °C, also prevents the identification of the cubic-pseudocubic transformation in the PMN sample. However, while the temperature ranges within which the onset of the cubic-pseudocubic transformation occurs are consistently greater than the respective T_m temperatures of the samples, it is significant to note that in all cases these temperature ranges include the respective T_{α} temperatures of the samples.

DISCUSSION

Since the broadened diffraction profiles shown in Fig. 3 indicate that the onset of the cubic to pseudocubic phase transformation may be associated with the temperature T_{α} at which the crystal lattice shows a marked increase in mechanical stiffness, it is of interest to plot the measured values of T_{α} on the "phase diagram" of the PMN-PT system developed by Choi et al. (1989) and Feigelson (2002) from measurements of T_m . It is evident that the limited number of measured T_{α} temperatures vary approximately linearly with increasing PT composition and produce a plot that is widely separated from the T_m plot at the composition of PMN, but draws closer to it with increasing composition and, if extrapolated, would intersect it in the region of the morphotropic phase boundary, near 30 mol.% PT. The values of T_{α} fall well below the temperatures of 343-345 °C at which Burns and Dacol (1983) infer that randomly oriented regions of polarization cease to exist in PMN, on the basis of refractive index measurements. There is a lack of precise data on the temperature $T_{P_s=0}$ at which saturation polarization goes to zero in relaxors,

but as this temperature it is generally considered to be no more than 100 °C above T_m (Cross, 1987, 1994), it is reasonable to associate it with the values of T_α , which are indicative of a stiffening of the crystal lattice. The lattice stiffening can thus be regarded as a necessary condition for the formation of stable oriented regions of polarization, which contribute to saturation polarization. The random orientation of these regions causes the structure to be macroscopically cubic, but of lower symmetry in the microregions, and thus gives rise to broadened cubic diffraction profiles.

The observation of distinct rhombohedral peaks at a temperature below T_m in the samples of 0.92PMN-0.08PT and 0.8PMN-0.2PT lends support to those who have suggested that the temperature T_f at which remanent polarization goes to zero should be used as the parameter to define the onset of the rhombohedral phase transformation (Viehland et al., 1990,1991). A study of the literature revealed a T_f value of -43 °C for PMN (Colla et al., 1999), but no data are available for the compositions of the other samples. However, values of 18 °C have been reported for 0.9PMN-0.1PT (Viehland, et al., 1991) and 70 °C for 0.8PMN-0.2PT (Guisheng, et al, 2000). Interpolating between these data gives T_f values in the region of 10 and 70 °C for the present 0.92PMN-0.08PT and 0.80PMN-0.2PT samples. It is significant to note that the published T_f value for PMN, and the interpolated values for the other PMN-PT samples, all lie within with the respective temperature ranges of -30 to -50°C, 10 to -10 °C and 80 to 60 °C, within which profile broadening associated with the onset of the rhombohedral phase is observed.

On the basis of the above discussion, a lower dashed line has been inserted into the phase diagram in Fig. 4, to indicate the temperature of the onset of the rhombohedral transformation, based on the published T_f values for PMN, 0.9PMN-0.1PT and 0.76PMN-0.24PT. The region of the diagram between the T_α and T_f plots is labeled "pseudocubic", but represents a two-phase region in which increasing amounts of

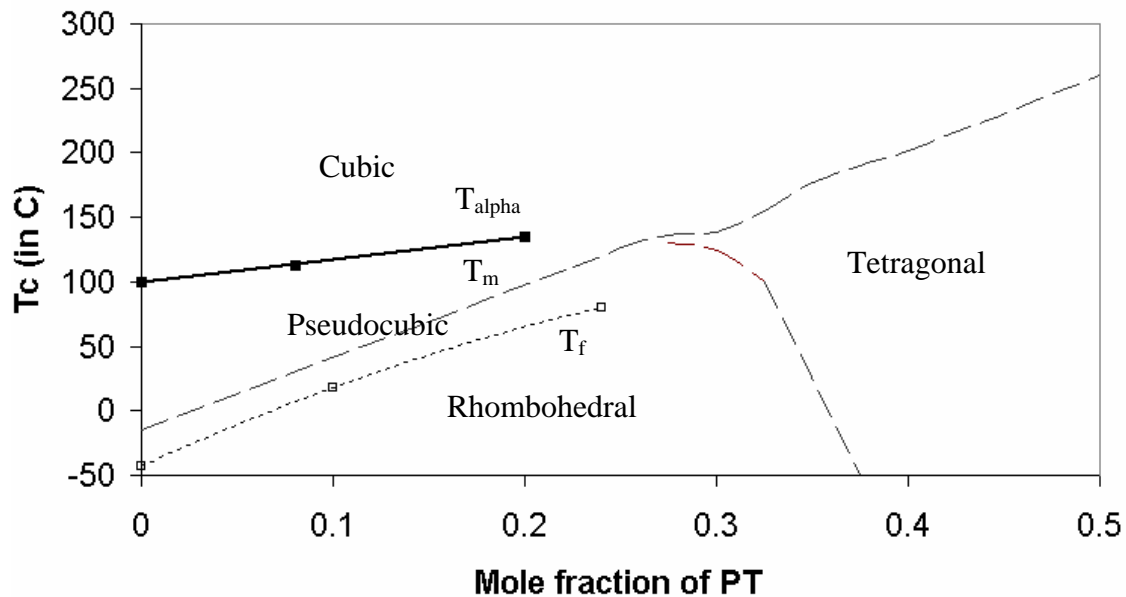


Figure 4. Relaxor region of the PMN-PT system.

randomly oriented polarization microregions are formed (athermally) as the temperature is lowered. The region below the T_f plot is labeled "rhombohedral" and represents a stable single phase region. The line T_m thus represents the temperature of the peak in dielectric constant, but has no significance as an indicator of a phase change in the relaxor region of the PMN-PT phase diagram. The modified phase diagram is only tentative at this stage and requires the addition of additional data points (derived from step scans of diffraction profiles using a smaller step size and a smaller temperature interval), in order to establish the phase boundary between the pseudocubic and rhombohedral phases more accurately. In addition similar experimentation must be performed at higher compositions in the region of the morphotropic phase boundary, to complete the phase diagram. Results of the latter experiments, which are in progress in the authors' laboratories, will be presented at the International Conference on Sonar-Sensors and Systems, to be held in Cochin, India, on December 11-13, 2002.

ACKNOWLEDGEMENTS

The authors acknowledge the support of the Natural Science and Engineering Research Council of Canada, the Office of Naval Research, USA, and the Department of National Defense, Canada.

REFERENCES

- Burns, G. and Dacol, F.H., (1983), *Solid State Commun.*, **48**(10), 853.
- Choi, S.W., Shrout, T.R., Jang, S.J. and Bhalla, A.S.,(1989), *Ferroelectrics*, **100**, 29.
- Colla, E.V., Furman, E.L., Gupta, S.M., Yushin, N.K., Viehland, D., (1999), *J. Appl. Phys.*, **85**(3), 1693.
- Cross, L.E., (1987), *Ferroelectrics*, **76**, 241.
- Cross, L.E., (1994), *Ferroelectrics*, **151**, 305.
- Feigelson, (2002), <http://www-mse.stanford.edu/people/faculty/feigelson/projects/PMNT/PMNhome>
- Guishing, X, Luo, H., Wang, P, Zhenyi, Q and Zhiwen, Y, (2000), *Chinese Science Bull.*, **45**(15), 1380.
- Ho, J.C., Liu, K.S. and Lin, I.N., (1993), *J. Mater. Sci.*, **28**, 4497.
- King, H.W., Peters, M.A., Payzant, E.A. and Stanley, M. B., (1994), *Adv. X-ray Anal.*, **37**, 457.

- King and Payzant, (2001), *Canad. Metall. Quart.*, **40**, 385.
- King, H.W., Yildiz, M, Ferguson, S.H., Waechter D.F. and Prasad, S.E., (2002), "X-ray Examination of the Phase Transition in Electrostrictive 0.9PMN–0.1PT", submitted to *Ferroelectric Letters*, September, 2002.
- de Mathan, N., Husson E., Calvarin G., Gavarrri J.R., Hewat A.W., Morell A., (1991), *J. Phys. Condens. Matter*, **3**, 8159.
- Schmidt, G., (1990), *Ferroelectrics*, **104**, 205.
- Schmidt, G., (1992), *Phase Transitions*, **20**, 127.
- Smolenski, G.A., Isupov, V.A., Agranovskaya, A.I. and Krainik, N.N., (1961A), *Soviet Physics - Solid State*, **2**(11) 2651.
- Smolenski, G.A., Krainik, N.N. and Agranovskaya, A.I., (1961B), *Soviet Physics - Solid State*, **3**(3), 714.
- Smolenski, G.A., Isupov, V.A., Agranovskaya, A.I. and Popov, S.N., (1961C), *Soviet Physics - Solid State*, **2**(11) 2584.
- Swartz, S.L., ShROUT, T.R., Schulze, W.A. and Cross, L.E., (1984), *J. Amer. Ceram. Soc.*, **67**, 311.
- Viehland, D., Li, J.F., Jang, S.J., Wuttig, M. and Cross, L.E., (1990), *J. Appl. Phys.*, **68**, 2916.
- Viehland, D., Li, J.F., Jang, S.J., Cross, L.E. and Wuttig, M., (1991), *Phys. Rev.*, **43B**(10), 8316.
- Waechter, D.F., Liufu, D., Camirand, M., Blacow, R. and Prasad, S.E., (2000), "Development of High-Strain Low-Hysteresis Actuators Using Electrostrictive Lead Magnesium Niobate (PMN)", *Proc. 3rd CanSmart Workshop Smart Materials and Structures*, p. 31.
- Westphal, V., Kleemann, Glinchuk, M.D., (1992), *Phys. Rev.*, **68**(6), 847.
- Zhang, Q.M., Zhao, J. and Cross, L.E., (1996), *J. Appl. Phys.*, **79**(6), 3181.
- Ye, Z.G. and Schmidt, H., (1993), *Ferroelectrics*, **145**, 83.